Nano-Structures & Nano-Objects 15 (2018) 153–166

Contents lists available at ScienceDirect

Nano-Structures & Nano-Objects

journal homepage: www.elsevier.com/locate/nanoso

2D nanomaterials assembled from sequence-defined molecules

Peng Mu [a,b], Guangwen Zhou [b], Chun-Long Chen [a,*]

[a] Physical Sciences Division, Pacific Northwest National Laboratory, Richland, WA 99352, USA
[b] Department of Mechanical Engineering and Materials Science and Engineering Program, State University of New York, Binghamton, NY 13902, USA

ARTICLE INFO

Article history:
Received 11 July 2017
Received in revised form 4 September 2017
Accepted 4 September 2017

Keywords:
2D nanomaterials
Sequence-defined molecules
Self-assembly
Surface chemistry

ABSTRACT

Two dimensional (2D) nanomaterials have attracted broad interest owing to their unique physical and chemical properties with potential applications in electronics, chemistry, biology, medicine and pharmaceutics. Due to the current limitations of traditional 2D nanomaterials (e.g., graphene and graphene oxide) in tuning surface chemistry and compositions, 2D nanomaterials assembled from sequence-defined molecules (e.g., DNAs, proteins, peptides and peptoids) have recently been developed. They represent an emerging class of 2D nanomaterials with attractive physical and chemical properties. In this mini-review, we summarize the recent progress in the synthesis and applications of this type of sequence-defined 2D nanomaterials. The challenges and opportunities in this new field are also discussed.

Contents

1. Introduction

Two dimensional (2D) nanomaterials have attracted increasing attention in recent decades owing to their unique structures and properties [1–5]. Graphene, as the first generation of 2D nanomaterials, was a groundbreaking discovery in materials science and soon became one of the most promising and versatile materials due to its unique structure and unusual properties [6]. The discovery of graphene 2D material was so meaningful in materials science history that its discoverers, Andre Geim and Konstantin Novoselov, were awarded the 2010 Physics Noble prize. Since then, a variety of structurally similar 2D nanomaterials have emerged [2,4], such as transition metal dichalcogenide nanosheets [2,7] and 2D polymers [8–11]. Despite the excellent physical and chemical properties of these 2D materials, they face challenges in tuning surface chemistry to achieve protein-like molecular recognition. Recently, scientists have managed to assemble functional 2D nanomaterials from sequence-defined molecules [1,12–19], such as DNAs [15,18,19], proteins [12,14], peptides [13] and peptoids (or poly-N-substituted glycine) [1,16,17] that have well-ordered structural skeletons and high information content encoded by the

* Corresponding author.
E-mail address: Chunlong.Chen@pnnl.gov (C.-L. Chen).

https://doi.org/10.1016/j.nanoso.2017.09.010
2352-507X/

sequence of side-chain residues. This type of 2D nanomaterials (or called sequence-defined 2D nanomaterials) has received increasing attention owing to their advantages in achieving tailorable and sequence-specific properties.

In this review, sequence-defined 2D nanomaterials will be mainly discussed in terms of their building block components, structural characterizations, and physical and chemical properties. After that, we will discuss some of their unique features which distinguish them from other 2D materials. In the end, we will summarize the features of this type of 2D nanomaterials and discuss their current challenges and promising applications.

2. Sequence-defined 2D nanomaterials

Sequence-defined molecules [1,12–19], such as DNAs [15,18,19], proteins [12,14], peptides [13] and peptoids, have recently been used as unique building blocks for assembly of 2D nanomaterials. Due to the sequence-specific molecular recognition of these functional building blocks, this type of 2D nanomaterials offers the potential to achieve high selectivity and easy surface tunability. Furthermore, they exhibit distinct features owing to the dramatic difference in the physical and chemical properties of their building blocks. Among these sequence-defined 2D nanomaterials, those assembled from peptoids are particularly interesting because they combine high stability and easy tunability [16].

2.1. DNA-based 2D nanomaterials

Due to the unique structural features and the self-recognition properties of DNA, several assembly strategies have been developed for building DNA-based 2D nanomaterials. Among them, the recently developed 'origami' method was found to be able to generate functional 2D nanostructures of arbitrary shapes, in which many of them were further used as nano-building blocks to assemble 3D nanostructures with high precision and specificity. For example, by using this approach, Liu et al. demonstrated the assembly of crystalline 2D DNA-origami arrays from two complementary cross-like DNA origami tiles [15]. Specifically, they first designed two types of origami tiles (A and B in Fig. 1(a)) whose helix axes propagate in two independent directions. These tiles have two distinct domains with orthogonal directions of propagation. After the individual cross-like origami tiles were formed, A and B tiles were mixed together and annealed to form a 2D DNA origami array (Fig. 1(b)). During this assembly process, the sequence-controlled complementary interactions played a critical role in the formation of crystalline 2D nanomaterials in which the coded information resulted in the selective attachment of sticky ends 1 and 2 in origami title A to 1′ and 2′ in title B (Fig. 1(a)); only annealing at 53 °C led to the successful assembly.

2D structures with various topologies have been assembled using a similar approach to design DNA origami tiles with other geometries and/or complementary interactions. For example, by having hexagonally-shaped DNA origami tiles, Wang et al. successfully assembled 2D honeycomb-like structures, in which DNA molecules were programmed specifically to fold into hexagonally-shaped origami tiles with six protruding arms in symmetric directions [18]. Each arm of these origami tiles was able to connect one origami tile, leading to the formation of a honeycomb-like 2D structure (Fig. 2(a)). By manipulating DNA sequences and modifying their chemistry, Suzuki et al. designed cross-like origami tiles exhibiting complementary interactions on all four edges [19]. These building blocks were able to assemble into a unique 2D nanostructure whose topology is distinct from those Fig. 1. In this case, the cross-like tiles are densely-packed to form a non-porous 2D nanostructure (Fig. 2(b)) [19].

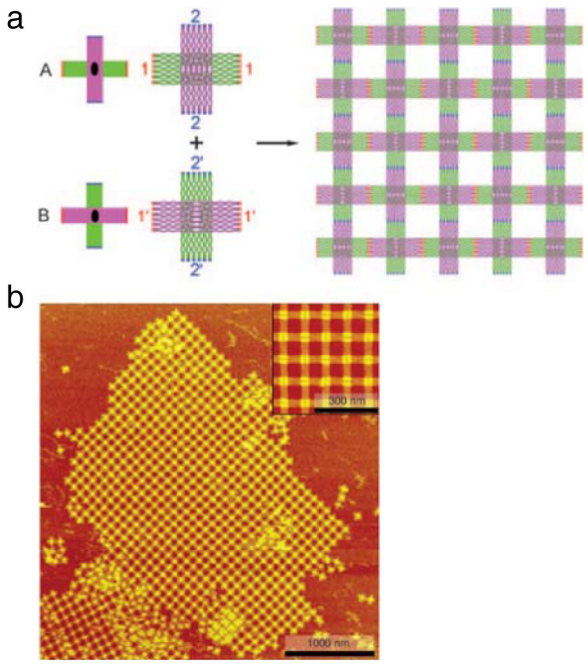

Fig. 1. (a) Two types of complementary DNA origami tiles (A and B) with orthogonal directions of propagation structure. (b) AFM image of a 2D origami array assembled from tiles A and B [15].

Despite the unique properties, DNA-based 2D nanomaterials are facing challenges in synthesis and applications. First, because of the sequence complexity of the DNA molecules, thousands of factors must be taken into account in designing DNA sequences, thus it is challenging to predict the assembly of DNA sequences into 2D nanomaterials. Recently, researchers rely heavily on computational calculations and simulations to determine whether desired structures can be created for newly designed DNA sequences [20]. Second, large DNA molecules are physically and chemically delicate and difficult to synthesize, so they generally cannot withstand harsh environments and the choice pool for input materials is limited [21]. Third, a large portion of sheet-forming DNA sequence binding sites are occupied for complementary interactions, thus surface decoration is difficult without disturbing the final 2D structures [21]. Last, the restriction to four base pairs severely limits the palette of potential materials and functionalities [22].

2.2. Protein-based 2D nanomaterials

Proteins, nature's most versatile building blocks, are programmed at the genetic level to assemble into molecular machines that carry out cellular functions and are largely responsible for the complexity of an organism. In these natural systems, the exquisite, error-free, and programmed self-assembly of proteins into ordered yet dynamic nano- and microscale architectures provides a route to patterning a large number of function groups at the atomic scale. Examples of 2D protein assemblies include crystalline bacterial cell surface layers [23]. The wide array of chemical functionalities provided by their 20 amino acid constituents enable protein assemblies to execute high-level functions. Inspired by nature, scientists have devoted tremendous efforts to exploit proteins as building blocks in the synthesis of functional materials, including 2D nanomaterials, because doing so will not only reveal natural design principles for protein self-assembly but also provide an opportunity to tailor materials with new physical and chemical properties. Over the last decades, a number of strategies have been devised for the assembly of proteins into 2D nanomaterials,

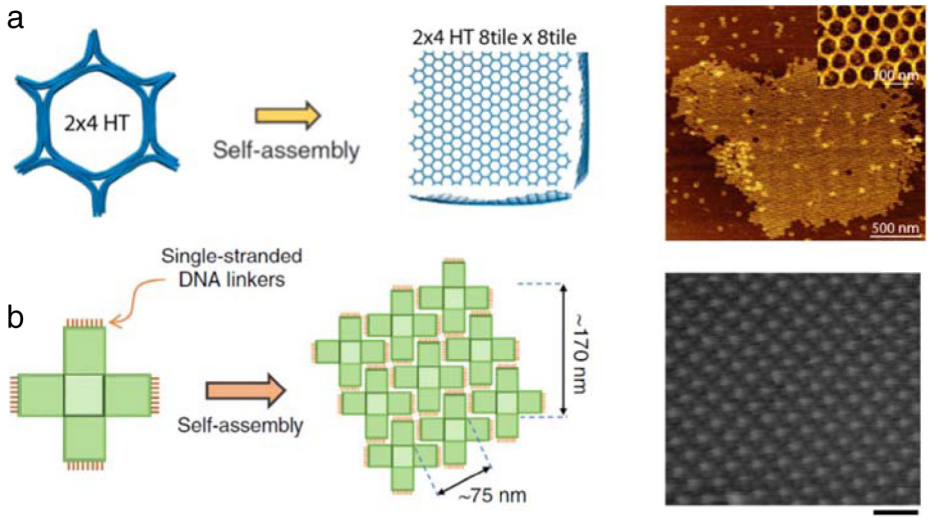

Fig. 2. (a) Assembly of DNA origami tiles with hexagonal geometries into a honeycomb-like 2D structure [18]. (b) Assembly of cross-shaped DNA origami tiles into a densely-packed 2D structure. Scale bar, 200 nm [19].

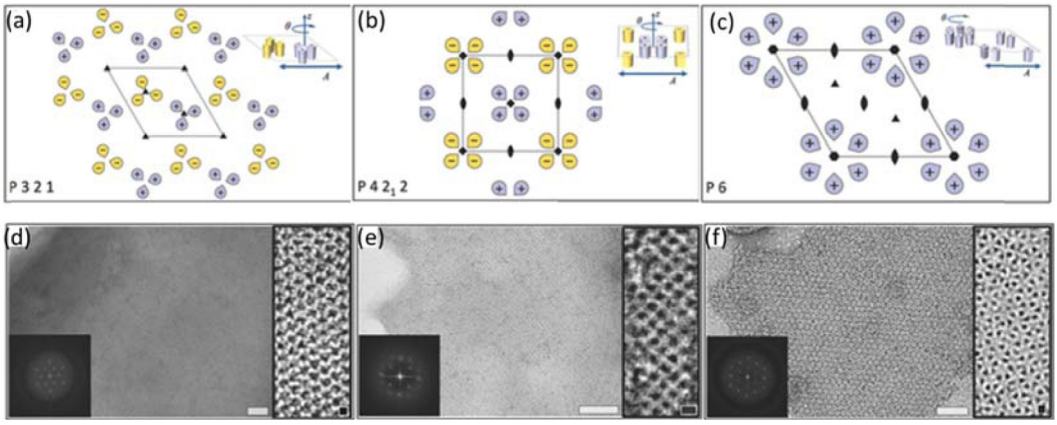

Fig. 3. Assembly of 2D protein arrays from computationally designed proteins with three distinct symmetries. (a, d) Proteins with a three-fold symmetry lead to the formation of a hexagonally-patterned 2D structure with a P 3 2 1 unit cell. (b, e) Proteins with a four-fold symmetry assemble into a 2D structure with the P 4 21 2 lattice. (c, f) Proteins with a six-fold symmetry lead to the formation of a 2D structure with the P 6 lattice. (d–f) Corresponding TEM images of the 2D protein arrays; high resolution images are in the right and the insets are Fourier transform images, All scale bars: black, 5 nm; white, 50 nm [24].

including the computational design of assembling proteins with shape-complementary interfaces pioneered by Baker's group [24], ligand-mediated assembly of protein building blocks without design of new protein–protein interactions [25], and assembly of protein building blocks using metal coordination [12,14,26], These approaches have successfully produced 2D nanomaterials with increasing structural sophistication and/or improved functions. For example, by computationally designing proteins that folded into specific symmetrical structures, Gonen et al. synthesized protein-based crystalline 2D nanomaterials that display different ordered and various periodic symmetries mediated by non-covalent protein–protein interactions [24]. As shown in Fig. 3(a), designed proteins with three-fold symmetry led to the formation of a hexagonally-patterned 2D structure with a P 3 2 1 unit cell (Fig. 3(a)), in which each charged protein building block is surround by three neighboring ones with opposite charges forming electrostatic interactions. Similarly, those with four-fold and six-fold symmetries assembled into 2D structures with a P 4 21 2 lattice and a P 6 lattice respectively. The resulting 2D nanomaterial morphologies were confirmed using TEM imaging (Fig. 3(d)–(f)).

By exploiting the strength, directionality, and reversibility of designed metal coordination interactions, Tezcan's group demonstrated the assembly of highly-crystalline 2D nanosheets from a monomeric, redox protein (cytochrome cb_{562}) [14,26]. They showed that the metal-directed assembly approach not only yielded stable architectures but also led to an improved stabilization of the individual protein components. Very recently, they further used this assembly approach to successfully synthesize dynamic 2D nanomaterials that underwent large-scale motions without loss of crystallinity [12].

Despite advances made in protein assembly, programmable control over protein self-assembly face significant challenges because proteins are complicated building blocks, which more often interact with each other and assembly in ways that are hard to predict [27,28]. Therefore, in comparison with DNA origami methods [22] that have been used to generate a wide variety of ordered structures, the progress in development of 2D protein assemblies is much slower.

2.3. Peptide-based 2D nanomaterials

Compared with proteins, peptides are less complex and consist of short amino acid sequences [29–31]. They exhibit protein-like molecular recognition and are able to self-assemble into 2D nanomaterials through formation of two different secondary structures, such as α-helices and β-sheets [13,30,32–34]. For example, by

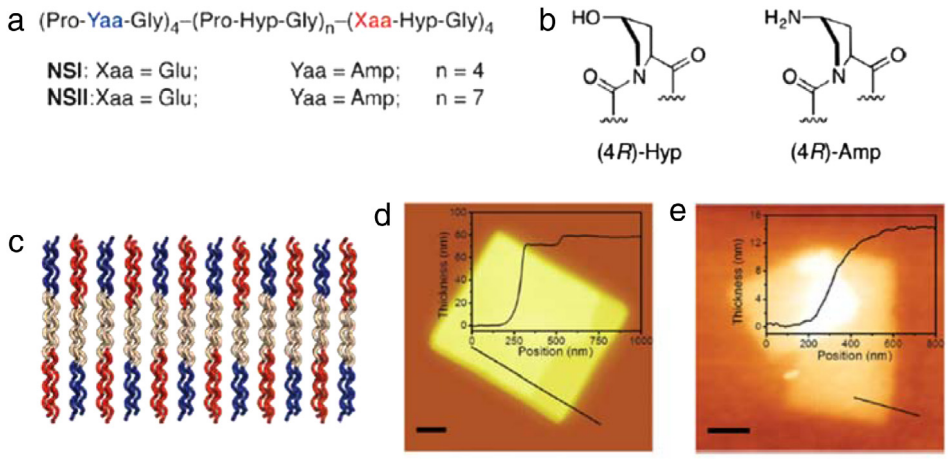

Fig. 4. (a) Peptide sequences NSI and NSII. (Red: negatively charged peptide residues; Blue: positively charged peptide residues.) (b) Structures of imino acid derivatives. (c) Proposed packing of collagen-mimetic peptide triple helices to form 2D nanomaterials, in which the triple helices are arranged together through electrostatic interactions. AFM images of NSI (d) and NSII (e) multilayer nanosheets with their inset height profiles, respectively (Scale bar: 200 nm) [13]. (For interpretation of the references to color in this figure legend, the reader is referred to the web version of this article.).

designing collagen-mimetic peptide triple helices NSI and NSII that form charge complementarity, Jiang et al. generated 2D nanomaterials with well-patterned charged residues through a layered packing of peptide triple helices [13]. Specifically, in order to assemble triple helices into 2D structures instead of fibrillary morphologies, NSI and NSII peptides were designed by incorporating structural features that promote selective interactions between triple helices. The high-level control over the assembly of nanosheets from NSI and NSII peptides indicates that sequence-defined molecules offer advantages as building blocks for building 2D nanomaterials with tunable surface chemistry and functional complexity. Furthermore, by designing peptides with different lengths and terminal functionalities, they were able to tune the nanosheet thickness (Fig. 4) [13].

However, due to their complex folding between backbones, the rational design and controlled synthesis of peptide assemblies is still underdeveloped, and the prediction of peptide self-assembly represents a formidable challenge. Therefore, though a large amount of 1D structures, such as nanofibers and nanoribbons, have been self-assembled [30], free-standing 2D nanomaterials based on peptides are rare [33], and the principles that govern their self-assembly into 2D materials are unknown. Besides the complexity of backbone folding of proteins and peptides, materials assembled from proteins or peptides often have challenges in technological applications owing to their poor chemical, thermal and biological stabilities [35].

2.4. Peptoid-based 2D nanomaterials

2D nanomaterials assembled from peptoids (poly-N-substituted glycine) are a type of newly-developed 2D materials that exhibit unique structural features and attractive properties. Peptoids are sequence-defined synthetic molecules that mimic both the structure and function of peptides and proteins, and bridge the gap between biopolymers and synthetic polymers [36]. They can be cheaply and easily synthesized and have large side-chain diversity. Furthermore, peptoids are biocompatible and show great promise for protein-like molecular recognition. Moreover, in contrast to peptides and proteins, they are highly thermally and chemically stable and offer the unique simplicity for self-assembly and tuning functions because they lack intra- and inter-molecular backbone hydrogen bonds [1,16,37,38]. Therefore, comparing to other types of sequence-defined 2D nanomaterials, those assembled from peptoids are much easier to synthesize and exhibit higher chemical and thermal stabilities, and their surface chemistry and interior core can be more easily tuned by changing peptoid side-chain chemistry [1,16].

2.4.1. Approaches to assembly of peptoid-based 2D nanomaterials

Two distinct approaches have been reported to assemble peptoids into 2D nanomaterials, depending on the structural features of peptoids:

(a) Assembly of nanosheets through an interface-assisted compression.

The assembly of amphiphilic peptoids into 2D nanosheets was first reported by Nam et al. in 2010; peptoids used in that study consist of alternating polar and nonpolar residues [39]. During the assembly process, soluble amphiphilic peptoids first present as globule structures, they then reach to the water–air or water–oil interface to exhibit an extended form [40] before they are compressed to form an ordered monolayers—a critical step for nanosheet formation [1,39,41]. Fig. 5 shows the assembly pathways of $(NpeNce)_7$-$(NpeNae)_7$ [Npe = N-(2-phenethyl) glycine (Npe), Nce = N-(2-carboxyethyl) glycine, and Nae = N-(2-aminoethyl) glycine] at the water–oil (Fig. 5(a)) [41] and water–air (Fig. 5(b)) [42] interfaces. Peptoids gather together at the interfaces with the hydrophilic Nce- and Nae-groups in the aqueous phase and the hydrophobic Npe-groups in the oil or air phases. They then align laterally at the interfaces to form ordered monolayers intermediates (Fig. 5(c)). During the assembly of these nanosheets, the hydrophobic interactions contribute significantly to sheet stability. The ordering of peptoids within nanosheets is determined largely during the monolayer formation. The monolayer formation rate is temperature dependent and increasing temperature accelerates the monolayer formation [43].

(b) Through a solvent-induced, spontaneous crystallization process.

By designing amphiphilic, lipid-like peptoids containing aromatic hydrophobic domains, we recently reported a facile solvent-induced crystallization approach to assembly of highly crystalline membrane-mimetic 2D nanomaterials (Fig. 6) [16,17]. In this case, the well-dissolved amphiphilic peptoids were first presented in solution as amorphous particles, they were then slowly crystallized to form elongated nanoribbons (Fig. 7(a)) as intermediates before they finally transformed into highly crystalline nanomembranes (Fig. 7(b)). The transformation of amorphous particles into highly crystalline nanomembranes was also confirmed by X-ray diffraction (XRD) data (Fig. 7(c)).

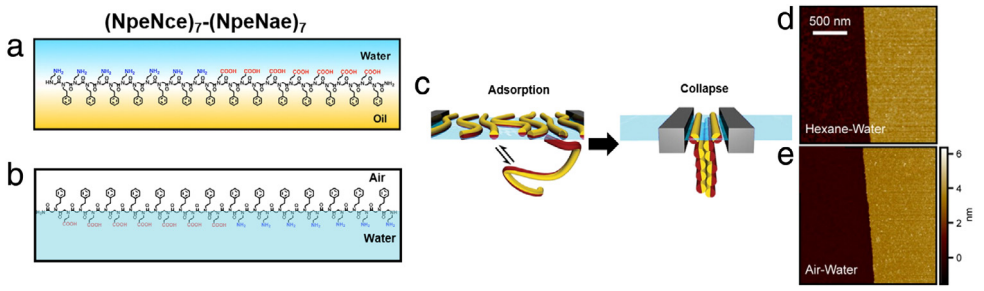

Fig. 5. Assembly of 28-mer peptoids into 2D nanosheets. (a) Schemes showing that the peptoid $(NpeNce)_7$-$(NpeNae)_7$ is trapped at the water–oil (a) and water–air interface (b). (c) The scheme showing the lateral alignment of amphiphilic peptoids at the interfaces before they are compressed to form bilayer nanosheets. AFM images of nanosheets formed through the water–oil (hexane) interface (d) or the water–air interface (e) [41,42].

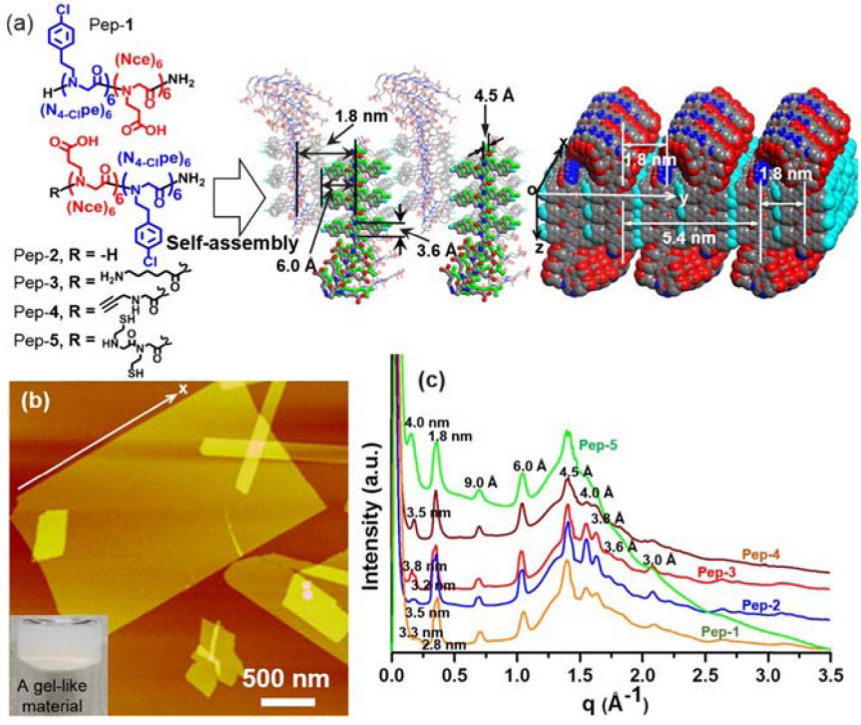

Fig. 6. (a) Structures of five membrane-forming peptoids and the scheme showing the assembly of these peptoids into 2D nanomembranes. (b) AFM image of Pep-1 nanomembranes, the inset is an optical image showing the gel-like material that contains a large amount of free-standing nanomembranes. (c) X-ray diffraction (XRD) data of nanomembranes assembled from Pep-1–Pep-5, showing that they are all highly crystalline and have similar structures [16].

During this assembly process, the presence of collective hydrophobic interactions (e.g. π-π interactions) contributes significantly to the formation of nanomembranes with high chemical and thermal stabilities [16]. Once the aromatic hydrophobic domain $(N_{4-Cl}pe)_6$ [N-[2-(4-chlorophenyl)ethyl]glycine] remains, a number of functional groups can be attached at the N-termini of membrane-forming peptoids (Fig. 6(a)) to generate membrane-mimetic 2D nanomaterials, in which lipid-like peptoids packed in an interdigitated way along both *x*- and *y* directions to form a lipid-membrane-like structure consisting of a hydrophobic interior and two polar faces (Fig. 6(a)). AFM data revealed that these peptoid-based 2D nanomaterials had straight edges (Fig. 6(b)) and exhibited a thickness in the range of 3.5–4 nm [16]. XRD data showed that nanomembranes assembled from Pep-1 to Pep-5 are highly crystalline and all exhibit similar structures (Fig. 6(c)), highlighting the potential of these 2D nanomembranes in tuning surface chemistry. There are several advantages about this type of the peptoid-based 2D nanomaterial system. First, the formation process is not limited in the use of the water–air or water–oil interface. Second, the peptoid building blocks are only 12–13mer long, which make these 2D nanomaterials easy to synthesize with low cost. Third, the direct crystallization approach allows introduction of functional objects through the co-crystallization approach (*vide infra*).

2.4.2. Tuning the surface chemistry and interior core of peptoid-based 2D nanomaterials

Due to the easy synthesis of peptoids, the surface chemistry and interior core of peptoids-based 2D nanomaterials can be precisely modified and tuned.

(a) Tuning surface chemistry of peptoid-based 2D nanomaterials.

Surface chemistry of peptoid-based 2D nanomaterials can be tuned by either changing the design of polar and nonpolar domains of peptoids or peptoid side-chain chemistry. For example, Zuckermann et al. demonstrated the assembly of giant nanosheets by mixing the negatively charged 36mer $(Nce–Npe)_{18}$ and positively charged 36mer $(Nae–Npe)_{18}$ in a molar ratio of 1:1 (Fig. 8) [39] The surface of these resulting nanosheets has a block charge array formed by alternating positively charged Nae and negatively charged Nce residues (Fig. 8(a)). These nanosheets are giant in size The edge dimension of these nanosheets can reach

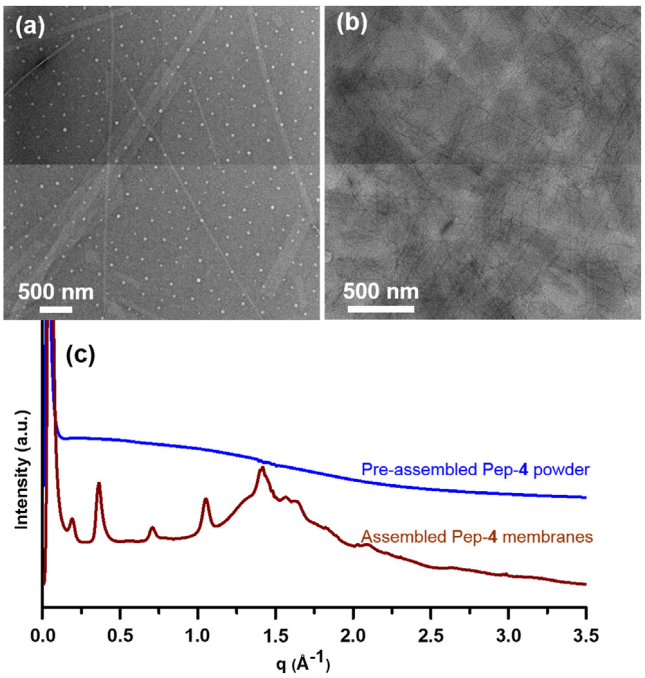

Fig. 7. (a and b) TEM images showing the anisotropic formation of peptoid-3 nanomembranes, in which both spherical particles and nanoribbons were observed after about one day (a); while well-defined 2D nanomembranes were formed after about two days (b). (c) XRD data of pre-assembled pep-4 powder and assembled membranes showing the transformation of amorphous aggregates into crystalline nanomaterials during the membrane formation process [16].

tens to hundreds of micrometers, as indicated by the fluorescent image of free-floating nanosheets stained with Nile Red dyes in aqueous solution (Fig. 8(d)). Later they further designed peptoids that contain both Nae and Nce groups and assembled nanosheets that exhibited a similar structure but a different surface chemistry (e.g. patterning of Nae and Nce groups) (Fig. 8(b)) compared to those assembled from mixed sequences [44]. Two-fold amphiphilic periodicity was used to design peptoids with charged residues alternatively positive and negative (alternating patterning) (Fig. 8(b)), or with charges segregated in positive and negative halves of the molecules (block patterning) (Fig. 8(c)). Both peptoids assembled into nanosheets, in which those with the alternating charges remained stable up to 20% acetonitrile, whereas sheets with the block pattern surface displayed greater robustness remaining stable up to 30% acetonitrile.

Tuning surface chemistry was also achieved for the crystallization-induced 2D nanomembrane system, in which once the hydrophobic domains $(N_{4-Cl}pe)_6$ remained, many variations can be applied to synthesize nanomembranes with tunable surface chemistry but exhibiting similar framework structures. For example, three peptoid sequences, as shown in Fig. 9, have the same $(N_{4-Cl}pe)_6$ hydrophobic blocks but with different hydrophilic groups, Nce_3, Nte_3 [Nte = N-2-(2-(2-methoxyethoxy)ethoxy)ethylglycine] and $(NceNae)_3$, respectively. All the three peptoid sequences assembled into 2D nanomembranes but exhibiting different surface chemistries [16].

(b) Tuning the interior core of peptoid-based 2D nanomaterials.

Because the ordering of hydrophobic domains is the key to forming and stabilizing peptoid-based 2D nanostructures, the interior core of this type of 2D materials can be adjusted by either modifying the hydrophobic side chains or introducing functional

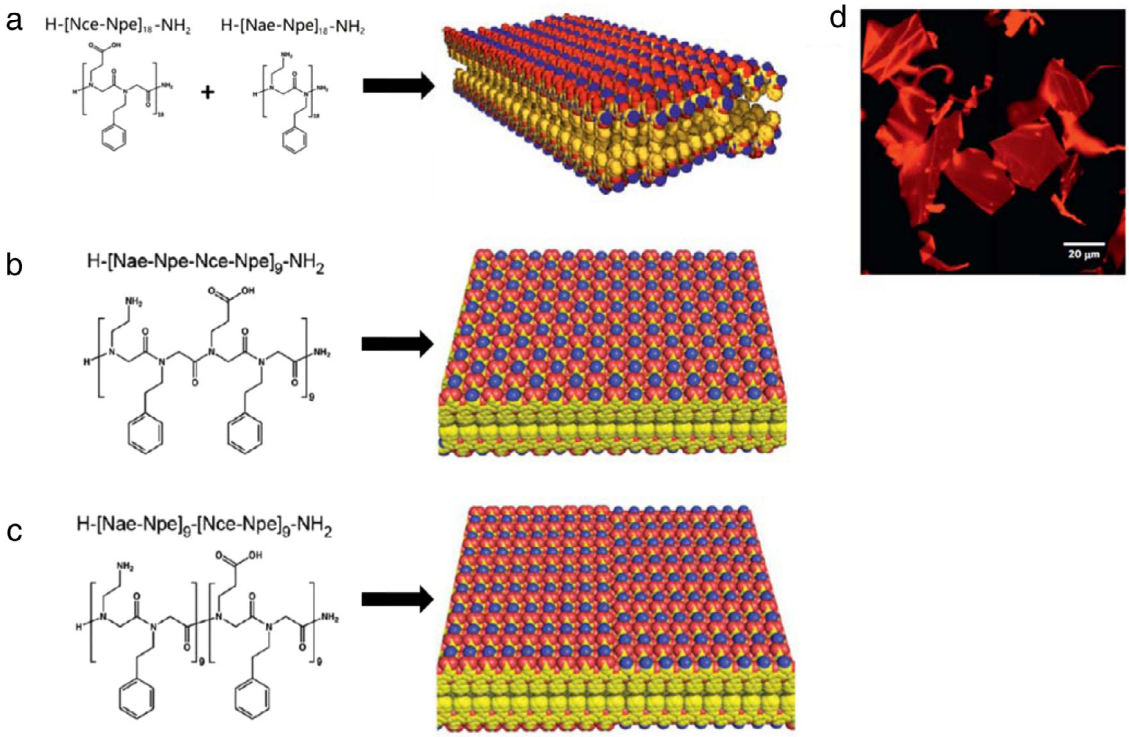

Fig. 8. (a) Structures of negatively charged $(Nce–Npe)_{18}$ and positively charged $(Nae–Npe)_{18}$ and their assembly into 2D nanosheets with a mixing ratio of 1:1 [39]. (b) Structure of alternating charge $(Nae–Npe–Nce–Npe)_9$ and its assembly into 2D nanosheets. (Red: negatively charged; Blue: positively charged. (c) Structure of block charge $(Nae–Npe)_9$-$(Nce–Npe)_9$ and its assembly into 2D nanosheets [44]. (d) Fluorescence image of giant nanosheets assembled from $(Nce–Npe)_{18}$ and $(Nae–Npe)_{18}$ with the molar ratio of 1:1; Nile Red dye was used to stain these free-floating nanosheets in aqueous solution [39]. (For interpretation of the references to color in this figure legend, the reader is referred to the web version of this article.)

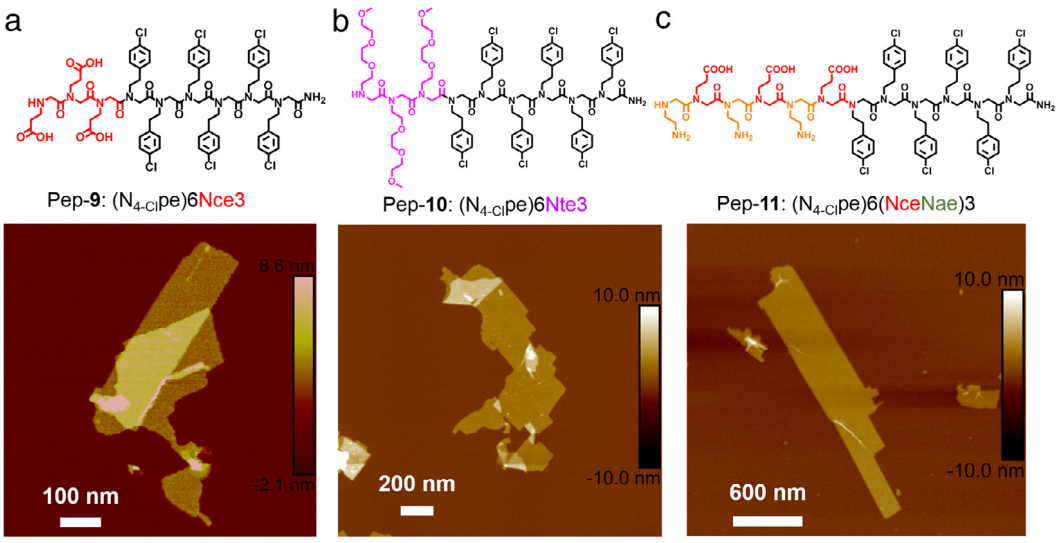

Fig. 9. Structures of three peptoid sequences (Top) and AFM images of their related nanomembranes (bottom) [16].

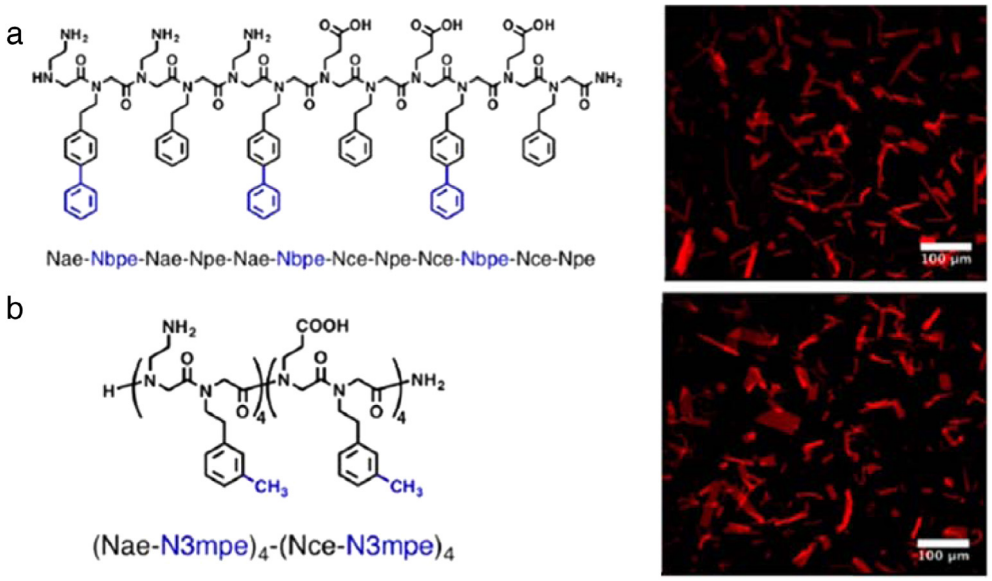

Fig. 10. Structures of peptoid sequences and fluorescence images of the Nile red stained nanosheets assembled from (a) 12mer peptoid Nae–Nbpe–Nae–Npe–Nae–Nbpe–Nce–Npe–Nce–Nbpe–Nce–Npe, and from (b) 16mer peptoid $(Nae\text{-}N3mpe)_4$-$(Nce\text{-}N3mpe)_4$ [45]. (For interpretation of the references to color in this figure legend, the reader is referred to the web version of this article.).

groups around the hydrophobic cores. For example, to assemble interface-induced nanosheets using shorter peptoid sequences, Robertson et al. [45] designed two peptoid sequences (Fig. 10(a) and (b)) with more hydrophobic side chains comparing to those reported previously [39,44]. As shown in Fig. 10, nanosheets with different interior cores were assembled from these 12-mer and 16-mer peptoids [45].

We recently demonstrated that 2D membranes from Pep-2 tolerated the incorporation of a wide range of functional objects as peptoid side chains (Scheme 1) and kept their overall structural framework intact [16]. The hydrophilic monomer Nte and the hydrophobic and electron-rich monomer Npyr (Scheme 1) were used as model objects to demonstrate the tolerance of incorporating highly hydrophilic and hydrophobic residues. Both resulting peptoids 13-Nte–Pep-2 (Nte is at the N-terminus of the peptoid as the 13th side chain) and 1-Npyr–Pep-2 (Npyr is located at the C-terminus as the 1st side chain) formed 2D membranes. XRD studies confirmed that they have similar and highly-crystalline structures (Fig. 11). Because Ntyr monomer (Scheme 1) mimics tyrosine—a redox-active residue significant for electron transfer during photosynthesis in nature [46] — We further demonstrated the successful incorporation of Ntyr at a number of locations to build 2D membranes with similar structures (Fig. 11). Some other functional objects (Scheme 1), such as Ntrp that mimics tryptophan—a redox-active residue that facilitates electron transfer [47], the azo-containing UV-responsive [48] Nazo monomer, and Nhis that mimics histidine—a residue significant for carbonic anhydrases to capture CO_2 [49], were also incorporated into assembled 2D nanomembranes using the same strategy. The consistency of all resulting structures suggests this peptoid assembly is robust to

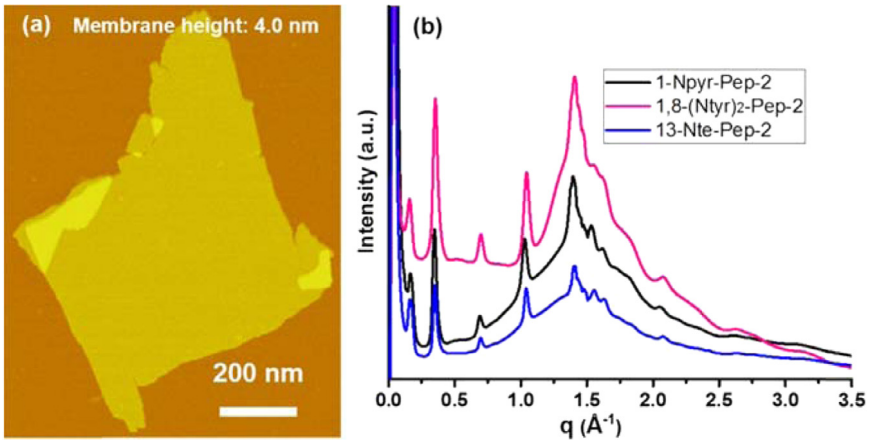

Fig. 11. Highly crystalline 2D membranes assembled from peptoids containing functional objects. (a) AFM image of one 2D membrane from 1-Npyr–Pep-2. (b). XRD data of membranes assembled from 1-Npyr–Pep-2, 1,8-$(Ntyr)_2$-Pep-2 or 13-Nte–Pep-2. They all exhibit similar XRD patterns, showing structural similarity [16].

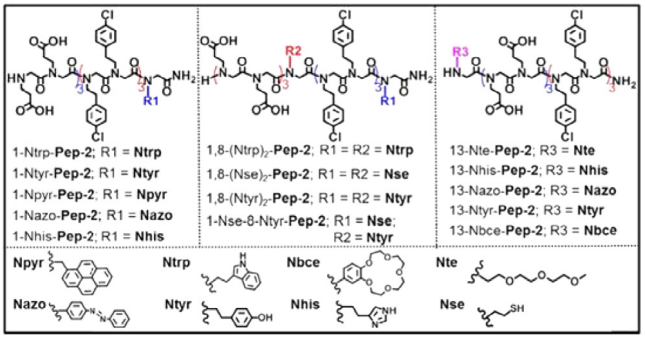

Scheme 1. Membrane-forming peptoids containing a wide range of functional objects as side chains [16].

tolerate the addition of model molecules and functional objects, resulting in nanomembranes with tunable interior cores.

2.4.3. Unique properties of peptoid-based membrane-mimetic 2D nanomaterials

2.4.3.1. The ability to self-repair. Because the structure of peptoid nanomembranes is similar to the packing of lipid bilayer, we recently demonstrated that these nanomembranes have the ability to self-repair [16,17]. To test that, we first deposited free-standing 2D nanomembranes on mica substrates and then created defects along three-different directions using AFM tips. By adding under-supersaturated free peptoid aqueous solutions and imaging the defects-containing peptoid membranes using *in situ* AFM, we were able to observe the self-repair of peptoid membranes in real time. Interestingly, the self-repairing process is anisotropic. As shown in Fig. 12, membranes exhibited the fastest repair rate along the *x*-direction [16].

To systematically investigate the repairing ability of peptoid nanomembranes and their repair mechanism, we performed self-repairing experiments for a range of substrates and solution conditions [17]. Our results demonstrated that peptoid membranes can self-repair on both positively and negatively charged hydrophilic surfaces, or without the support of surfaces. Membrane repair rates are anisotropic. Membrane repairs in either direction and during either stage of repair could be altered by changing the peptoid concentration or the solution pH. In specific, the free-standing membranes were deposited on substrates comprised of either atomically flat hydrophilic mica with positively or negatively charged surfaces, or highly ordered pyrolytic graphite (HOPG), which is hydrophobic. After creating defects on these as-deposited membranes using AFM tips with a vertical load greater than ≈10 nN, solutions containing peptoids in monomeric form were introduced to the AFM fluid cell to monitor the repair process in real time. We found defects-containing Pep-3 membranes fully repaired within 40 min after they were exposed to 10×10^{-6} M Pep-3 solutions at pH 2.6. Under this condition, the repair along the *x*-direction was faster than along the *y*-direction. When solution pH was increased to 4.3, Pep-3 repair rates dropped significantly and two distinct phases of repair were observed along both the *x*- and *y*-directions. The repair during the first stage was an order of magnitude slower than during the second stage. Because the COOH group side chains probably have different charge states when the solution was changed from pH2.6 to pH4.3, we reasoned that the slower repair rates were due to the inter-monomer electrostatic repulsion. When the mica surface was changed to positively charged, repair rates along both *x*- and *y*-directions were increased. While repair rates only increased slightly, the repair rate during the first stage along the *x*-direction increased by over 400%. We reasoned that the electrostatic attraction between the COO^- group and the positively charged surface contributed significantly to the observed increase repair rate [17].

By depositing a stack of two Pep-3 membranes onto a HOPG surface (Fig. 13), though the first layer of membranes directly contacted with the HOPG surface could not be repaired possibly due to a major change in conformation, we observed the repair of the second layer of defects-containing membrane that has no direct contacts to the HOPG surface, both at pH 2.6 and pH 4.3. These results demonstrated that the self-repair of peptoid membranes could happen in bulk solution—i.e., in the absence of a substrate [17].

2.4.3.2. Incorporation of bulky functional objects through a co-crystallization method. Because the peptoid nanomembranes were formed through a solvent-induced crystallization process, this system has the unique co-assembly capability in introducing bulky functional objects, in which the related peptoids were mixed with membrane-forming sequences in the early stage of the crystallization process. As shown in Fig. 14, Ncd–Pep-2 itself only assembled into one-dimensional (1D) nanoribbons (Fig. 14(b)). When it was mixed with membrane-forming Pep-2 in an 1:4 molar ratio, the resulting mixture led to the formation of only 2D nanomembranes (Fig. 14(c)). XRD data confirmed that these resulting Ncd-containing membranes had the same framework structures of Pep-2 nanomembranes. By varying the molar ratios of Ncd–Pep-2 and Pep-2, we further demonstrated the capability of tuning the density of Ncd residues within nanomembranes [16].

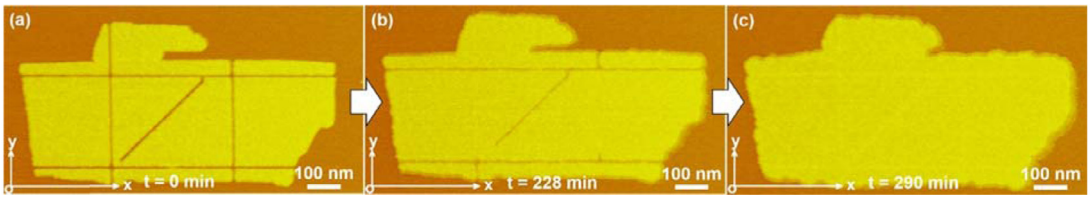

Fig. 12. Pep-3 membrane self-repairs. (a–c) *In situ* AFM images showing the anisotropic self-repair of one membrane with mechanically-induced defects, in which membrane exhibited the most rapid repair along the *x*-direction [16].

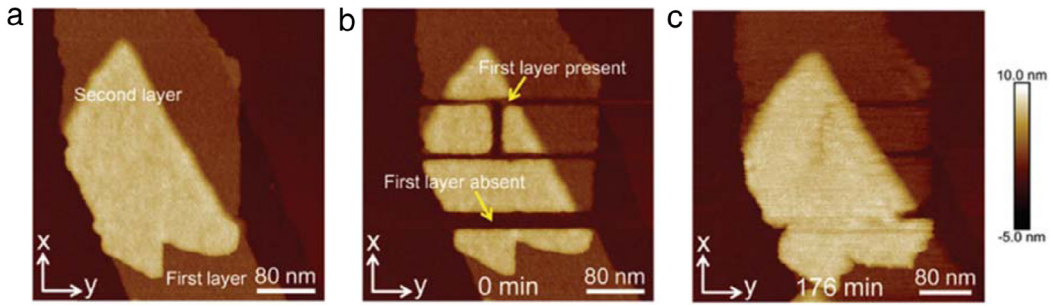

Fig. 13. (a–c) *In-situ* AFM images showing the self-repair of peptoid membranes in the absence of a substrate, in which a stack of two Pep-3 membranes were deposited on the HOPG surface and defects along *x*- and *y*-directions were introduced using AFM tips. The repairing results demonstrated the successful repair of the upper Pep-3 membranes [17].

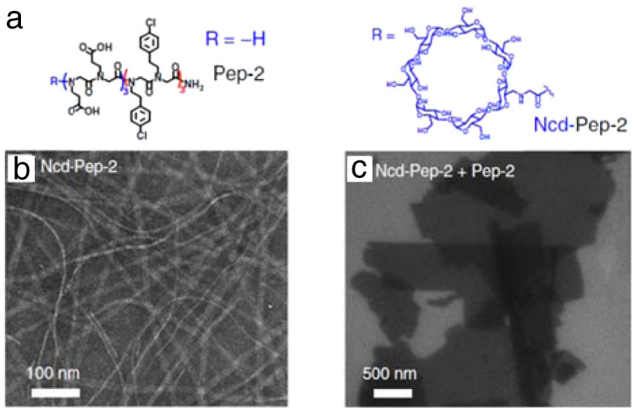

Fig. 14. Introducing bulky functional objects through co-crystallization. (a) Chemical structure of two peptoid sequences, Pep-2 and Ncd–Pep-2. (b) TEM image of self-assembled Ncd–Pep-2 nanoribbons. (c) SEM image of 2D membrane co-crystallized from Pep-2 and Ncd–Pep-2 (molar ratio: 1:4) [16].

2.4.3.3. Nanoscale patterning of functional objects within 2D nanomembranes. Because nanomembrane synthesis is driven by the interactions between phenyl rings within the hydrophobic core [16], we demonstrated that the repair of defect-containing nanomembranes using peptoids that possess identical hydrophobic domains but have functional objects at the hydrophilic block. As a result of such repairing process, we were able to achieve the nanoscale patterning of functional objects within nanomembranes [16,17]. For example, as shown in Fig. 15, when Pep-3 nanomembranes with cross-like defects were mixed with NHS-Rhodamine-labeled Pep-3, we demonstrated the nanoscale patterning of Rhodamine dye molecules within peptoid nanomembranes [16]. Similarly, we were able to achieve nano-patterning of a wide range of functional objects within peptoid nanomembranes [16,17].

2.4.3.4. Peptoid nanomembranes exhibit high stability and salt-induced thickness variations. Due to the enhanced packing among hydrophobic domains, peptoid-based nanomembranes survived from heating and within organic solvents [16]. As shown in Fig. 16,

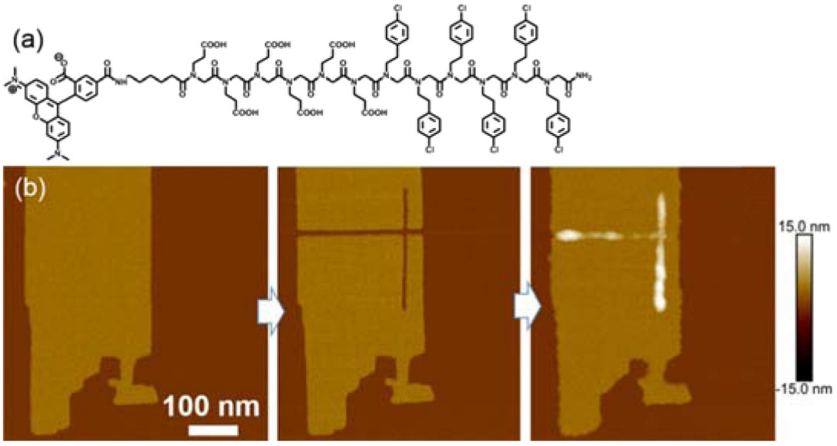

Fig. 15. (a) Structure of NHS-Rhodamine–Pep-3. (b) The repair of defect-containing Pep-3 nanomembranes with NHS-Rhodamine–Pep-3 created the cross-like patterning of Rhodamine dye molecules within one Pep-3 nanomembrane [16].

AFM results show these 2D nanomembranes are highly stable and exhibit almost no changes after being placed in a mixture of water and organic solvents, or even in pure organic solvents (e.g., EtOH or CH_3CN). We found that they also survived after heating to 60 °C overnight in water (Fig. 16(a)), being immersed in 10× PBS buffer solution for 3 h (Fig. 16(b)), in pure ethanol for 6 h (Fig. 16(c)), or in 1.0 M Tris–HCl buffer solution for 3 h (Fig. 16(d)).

Another unique feature of these nanomembranes is the ability to undergo thickness variations upon salt concentration changes, behaving like cell membranes. As shown in Fig. 16(e), when Pep-3 membranes were exposed to the solutions of NaCl or PBS buffer at different concentrations, peptoid membranes became thicker when the concentration of NaCl or PBS increased; membrane thicknesses were varied from ∼ 4.2 nm to ∼ 5.4 nm [16].

Taken together, peptoid-based membrane-mimetic 2D nanomaterials exhibit unique features by combining advantages of 2D nanomaterials (e.g., high surface area) and high side-chain diversity of protein and peptide-based materials. Moreover, they exhibit a number of properties associated with cell membranes, including thicknesses in the 3.5–5.6 nm range, spontaneous assembly at interfaces, thickness variations in response to changes in Na^+ concentrations, and the ability to self-repair. Furthermore, they are superior to lipid bilayers and other membrane-mimetic 2D nanomaterials assembled from lipid analogues because: (1) they are highly stable, free-standing, and atomically ordered; (2) attaching a broad range of functional objects at various locations in the peptoid sequence leaves this basic membrane structure intact; and (3) they serve as a robust platform to incorporate and pattern functional objects through large side-chain diversity and/or co-crystallization approaches. Given that peptoids are sequence-specific, highly stable, biocompatible, and exhibit protein-like molecular recognition, we believe membrane-mimetic 2D nanomaterials represent a significant step in the development of biomimetic membranes for applications in water purification, surface coatings, biosensing, energy conversion, or biocatalysis.

3. Applications of sequence-defined 2D nanomaterials

3.1. As templates to control the formation and assembly of inorganic crystals.

Due to the unique molecular recognition and tunable surface chemistry, 2D nanomaterials assembled from sequence-defined molecules offer advantages as templates to control the formation and assembly of inorganic crystals. For example, because the negatively charged C-terminal carboxylate groups are expected to interact selectively with the positively charged ammonium ion immobilized on the gold nanoparticles, Jiang et al. used nanosheets assembled from NSII peptides as templates for the packing of gold nanoparticles at the surfaces of NSII nanosheets (Fig. 17(a)) [13]. Wang et al. demonstrated the utilization of DNA origami based nanosheets for templating the organization of plasmonic gold nanoparticles. Owing to the hexagonal patterns of the DNA origami 2D nanostructure, gold nanoparticles were captured in the intratile hexagonal cavities at the center of each DNA origami tile, resulting in the formation of particle assemblies with a highly regular lattice structure (Fig. 17(b)) [18]. By taking advantages of the protein-directed reduction of surface-attached Pt^{2+} into Pt nanoparticles, Brodin et al. demonstrated that RIDC3 protein nanosheets could direct the formation of 2D assemblies of dendritic Pt^0 nanoparticles (Fig. 17(c)) at room temperature and 2D assemblies of Pt^0 single particles at 99 °C (Fig. 17(d)) [50].

Inspired by the hierarchical structures and enhanced mechanical performance of Nacre, recently, Zuckermann et al. used peptoid nanosheets as templates to control the formation of calcium carbonate materials, in which the amorphous calcium carbonate particles were grown at the binding sites on both sides of peptoid nanosheets [51].

3.2. As bio-inspired catalysts

Bio-inspired catalysis is another application of this type of sequence-defined 2D nanomaterials. For example, Jang and colleagues recently developed a type of tyrosine-containing 2D nanosheets assembled from peptide YYACAYY (Fig. 18(a)). Because tyrosyl radicals can be generated from tyrosine residues for catalytic formation of polypyrroles, they deposited both peptide nanosheets and tyrosine monomers in fluorine-doped tin oxide (FTO) substrates and applied a potential of 0.9 V versus the normal hydrogen electrode (NHE). As shown in Fig. 18(b), while there was almost negligible amount of polypyrrole deposition on the tyrosine-monomer-deposited FTO substrate, the black polypyrrole film was deposited continuously for the FTO decorated with peptide nanosheets. These results indicated that peptide nanosheets were able to produce highly-ordered tyrosyl radicals that were stable and active in the catalytic reaction media where monomeric ones could be easily quenched [52]. This study highlights the potential of using sequence-defined 2D nanomaterials to precisely pattern and stabilize catalytic sites for achieving highly effective catalysis.

3.3. As enhancers in boosting retroviral transduction

Recently, Dai et al. demonstrated the assembly of 2D nanosheets from KLVFFAK—a key amyloid-forming heptapeptide of the Italian familial form of Alzheimer's Aβ [33]. These nanosheets contained a major content of antiparallel β-sheets and featured most of the typical amyloid characteristics. Lysine residues at the peptide termini localized on the nanosheet surfaces, resulting in both sides of nanosheets highly positively charged. Because amyloid fibrils with similar positively charged surfaces could mediate HIV infection and laboratorial retroviral gene transfer [53], they further tested these amyloid-like nanosheets for viral infection. Interestingly, these nanosheets significantly enhanced lentiviral infection of HEK293T cells, and they were much more effective than the commonly used polybrene enhancer and the KLVFGAK fibril (Fig. 19), suggesting the nanosheet morphology is the key. Nanosheets provide surfaces large enough to support viral attachment, while fibrils are too thin for catching virus [33]. By tuning the surface chemistry of peptide nanosheets while the "LVFFA" core sequences responsible for nanosheet assembly were remained, they demonstrated that having positively-charged surfaces is significant for the enhanced effect on retroviral transduction [33].

3.4. As antibody-mimetic materials

Sequence-defined 2D materials can be synthesized and engineered as antibody-mimetic materials for molecular recognition, in which a high density of conformationally constrained loops can be displayed on both surfaces of free-floating nanosheets [54]. For example, due to the highly stability of peptoid nanosheets, Zuckermann et al. recently designed loop-containing peptoids and assembled them into antibody-like nanosheets: sheets decorated with surface-exposed loop domains [54]. They demonstrated that chemically diverse loops can be readily displayed at high density on the nanosheet surfaces. Specifically, peptoid loops and biologically active peptides were inserted in the middle of the linear peptoid sequences, between two amphiphilic sheet-forming domains (Fig. 20(a)). After compression of these loop-containing peptoids, the amphiphilic domains were aligned and packed tightly with the loops stood out on the surfaces (Fig. 20(b)). AFM results confirmed that the nanosheets assembled from loop-containing peptoids are thicker and have higher surface roughness than those assembled

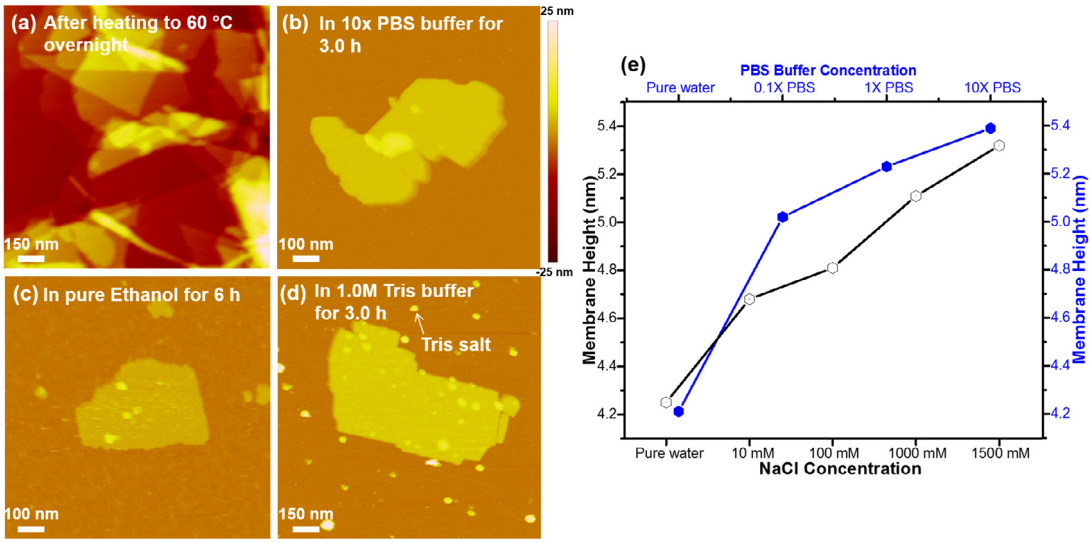

Fig. 16. Peptoid membranes are highly stable and dynamic. (a)–(d) AFM results showing the high stability of peptoid membranes against heating and chemical incubations. (e) The thickness of Pep-3 nanomembranes increased as the salt concentration increased [16].

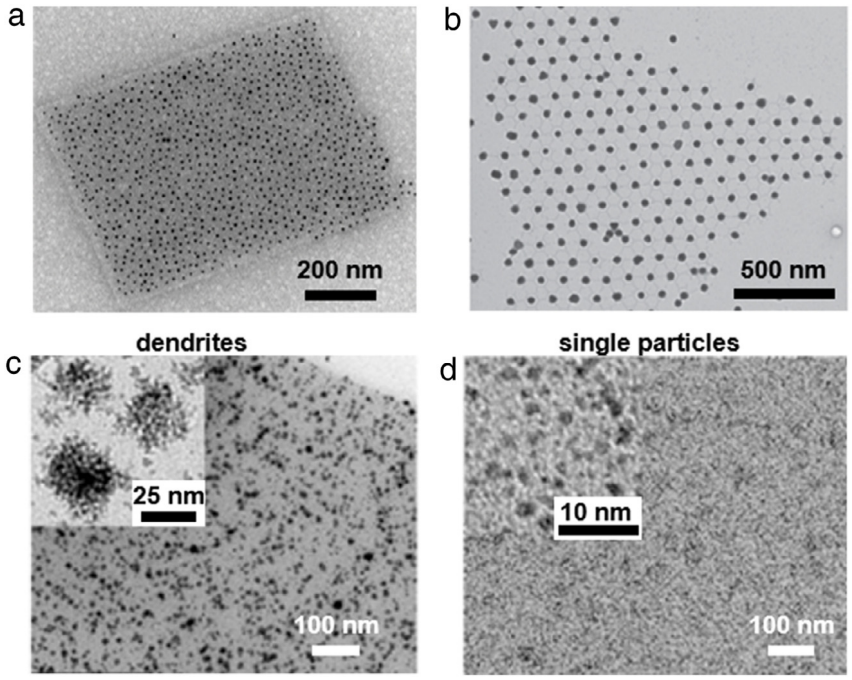

Fig. 17. TEM images of (a) peptide nanosheet NSII with gold nanoparticles spread out evenly (scale bar, 200 nm) [13], (b) 30 nm gold nanoparticles deposit on a hexagonal patterned 2D DNA origami nanosheet [18], (c) & (d) Pt nanoparticles spread out on a 2D RIDC3 protein nanosheet with insets showing (c) the formed dendrites at room temperature and (d) single particles reduced at 99 °C [50].

from non-loop containing sequences. By mixing specific peptide-loop displaying nanosheets with enzymes Pronase or casein kinase II (CK2α), they demonstrated these antibody-mimetic nanosheets were capable of molecular recognition of enzymes. For example, when these nanosheets were incubated with Pronase, AFM images (Fig. 20(c)) and mass spectrometry (MS) data confirmed the digestion of peptide loops displayed on nanosheets, demonstrating the peptide loops are accessible for recognition and cleavage by proteases. Meanwhile, the nanosheet substrate remains intact, demonstrating the enzyme stability of peptoid-based 2D nanomaterials (Fig. 20(c)) [54].

By inserting AD peptoid 3 (ADP3), a peptoid that was known to detect AD serum through identifying Aβ42, into the sheet-forming peptoid [55], Zhu et al. demonstrated the assembly of 2D nanosheets with ADP3 loops exposed on both surfaces (Fig. 21(a)) [56]. AFM images showed that these loop-containing nanosheets were much rougher in contrast to those without loops. While loop-absent nanosheets had a thickness of $\sim$ 2 nm, those containing ADP3-loops had a thickness of 5–6 nm (Fig. 21(b)) [56]. After immobilizing these ADP3-loop-displaying nanosheets on the 3D sensor chips, the resulting nanosheet functionalized chips were used to detect AD serum through surface plasmon resonance imaging (SPRi). They demonstrated that these ADP loop-containing nanosheets enhanced the capture efficacy of Aβ42 on the sensor surface and were able to identify AD sera with high sensitivity. As shown in Fig. 21(c), ADP3 loop-displaying nanosheets significantly detected AD sera from the normal ones even at the dilution ratio

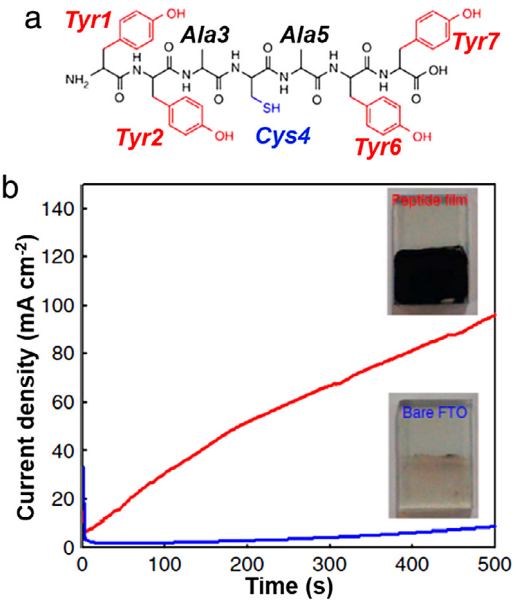

Fig. 18. (a) Structure of peptide YYACAYY. (b) The current density profiles of YYACAYY nanosheet (red) and tyrosine monomer (blue) deposited on tin oxide substrates (FTO) substrates during bulk electrolysis at 0.9 V in 0.1M NaCl containing 50 mM pyrrole. After 30 mins of reactions, while almost no polypyrroles were observed for monomer-deposited FTO, nanosheet-deposited FTO became black and were covered with polypyrroles [52]. (For interpretation of the references to color in this figure legend, the reader is referred to the web version of this article.).

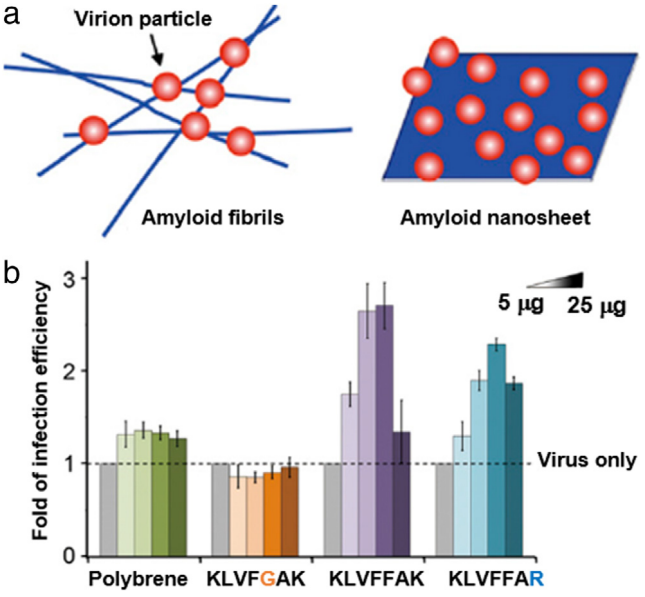

Fig. 19. (a) Schemes showing the attachment of virus particles on fibrils and nanosheets with positively-charged surfaces. (b) The retroviral transduction enhancing efficiency by using polybrene, KLVFGAK nanofibril, KLVFFAK, and KLVFFAR nanosheets [33].

of 1:8000 — an unprecedented dilution ratio for most of biosensors (Fig. 21(c)) [56].

4. Summary and outlook

As discussed above, owing to the unique structural features and properties of 2D nanomaterials assembled from sequence-defined molecules, there has been considerable interest in development of this type of 2D nanomaterials. The high-information content

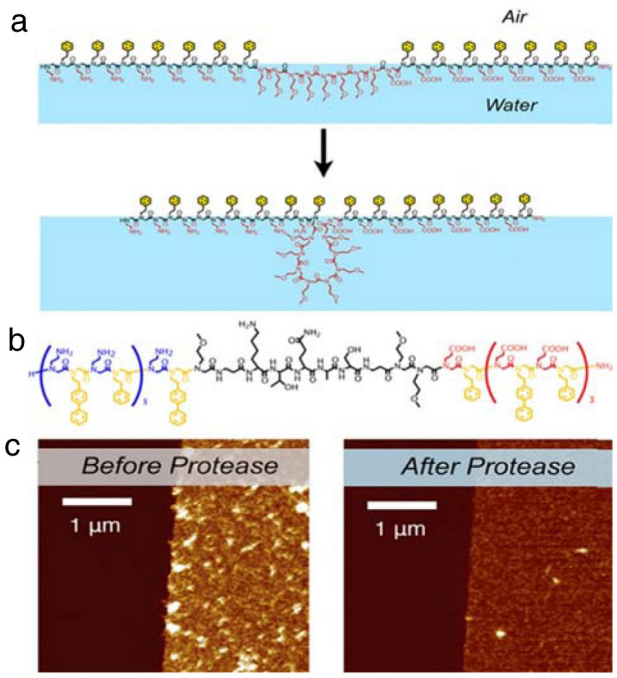

Fig. 20. (a) Schemes showing the compression of a peptoid loop-containing linear peptoid sequence at air/water interface. (b) Chemical structure of a peptide loop-containing peptoid sequence. (c) AFM images of one nanosheet assembled from sequence in (b) before and after protease-induced digestion of peptide loops [54].

of building blocks offer great potential of these sequence-defined 2D nanomaterials in applications varied from molecular sensing to biomedicine. In particular, peptoid-based 2D membrane-mimetic nanomaterials are attractive because they combine the advantages of peptide- and protein-based 2D nanomaterials (e.g. highly designed diversity and functionalities) and the conventional 2D nanomaterials (e.g., high chemical and thermal stability). Therefore, they have a bright future in biotechnology applications. Besides, the co-crystallization approaches and self-repair capability make them promising in building artificial membranes for ion transport and water purification. However, despite significant progress has been made in developing sequence-defined 2D nanomaterials, the synthesis and applications of these 2D nanomaterials are still at their early stages, and achieving the predictive synthesis of this type of materials with controllable functions is still a big challenge. In fact, scientists are still struggling with establishing the fundamental principles that underline the assembly of sequence-defined molecules into 2D nanomaterials. Specifically, the mechanism of the self-assembly process and how the sequence and side chains influence the 2D nanomaterial formation and materials function are still elusive. Although there is still a long way to go to fully understand the fundamental principles of the self-assembly process and how the various side chains affect the materials stability and self-assembly behavior, advances in both *in situ* molecular imaging [16,38,57] and computational simulations [16,38,58,59] offer us opportunities to understand assembly pathways and dynamics and determine physical parameters (e.g., free energy and kinetic barriers) that control assembly. The fusion of experimental efforts with extensive computational simulations will enable the rational design of sequence-defined 2D nanomaterials with tunable compositions and predictable functions.

Acknowledgments

This work was supported by the Materials Synthesis and Simulation Across Scales (MS3) Initiative through the LDRD fund at

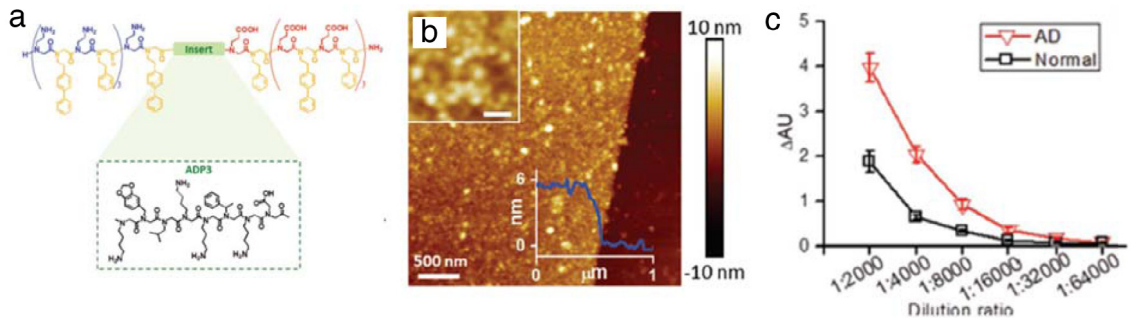

Fig. 21. (a) Structure of the ADP3 loop-containing sheet-forming peptoid. (b) AFM image and height profiles of ADP3 loop-containing nanosheets. Inset: the magnified image showing individual loops. (Scale bar: 100 nm) (c) SPRi binding signals of ADP3 loop-displaying nanosheets to AD and normal sera at different dilution ratio [56].

Pacific Northwest National Laboratory (PNNL). PNNL is multi-program national laboratory operated for Department of Energy by Battelle under Contracts No. DE-AC05-76RL01830.

References

[1] E.J. Robertson, A. Battigelli, C. Proulx, R.V. Mannige, T.K. Haxton, L.S. Yun, S. Whitelam, R.N. Zuckermann, Design, synthesis, assembly, and engineering of peptoid nanosheets, Acc. Chem. Res. 49 (3) (2016) 379–389.
[2] C.L. Tan, H. Zhang, Two-dimensional transition metal dichalcogenide nanosheet-based composites, Chem. Soc. Rev. 44 (9) (2015) 2713–2731.
[3] Y.Q. Guo, K. Xu, C.Z. Wu, J.Y. Zhao, Y. Xie, Surface chemical-modification for engineering the intrinsic physical properties of inorganic two-dimensional nanomaterials, Chem. Soc. Rev. 44 (3) (2015) 637–646.
[4] G.R. Bhimanapati, Z. Lin, V. Meunier, Y. Jung, J. Cha, S. Das, D. Xiao, Y. Son, M.S. Strano, V.R. Cooper, L.B. Liang, S.G. Louie, E. Ringe, W. Zhou, S.S. Kim, R.R. Naik, B.G. Sumpter, H. Terrones, F.N. Xia, Y.L. Wang, J. Zhu, D. Akinwande, N. Alem, J.A. Schuller, R.E. Schaak, M. Terrones, J.A. Robinson, Recent advances in two-dimensional materials beyond graphene, ACS Nano 9 (12) (2015) 11509–11539.
[5] X.M. Sun, Z. Liu, K. Welsher, J.T. Robinson, A. Goodwin, S. Zaric, H.J. Dai, Nano-graphene oxide for cellular imaging and drug delivery, Nano Res. 1 (3) (2008) 203–212.
[6] A.K. Geim, K.S. Novoselov, The rise of graphene, Nature Mater. 6 (3) (2007) 183–191.
[7] K. Kang, K. Godin, Y.D. Kim, S. Fu, W. Cha, J. Hone, E.H. Yang, Graphene-assisted antioxidation of tungsten disulfide monolayers: Substrate and electric-field effect, Adv. Mater. 29 (18) (2017) 1603898.
[8] J.W. Colson, W.R. Dichtel, Rationally synthesized two-dimensional polymers, Nature Chem. 5 (6) (2013) 453–465.
[9] W. Liu, X. Luo, Y. Bao, Y.P. Liu, G.-H. Ning, I. Abdelwahab, L. Li, C.T. Nai, Z.G. Hu, D. Zhao, B. Liu, S.Y. Quek, K.P. Loh, A two-dimensional conjugated aromatic polymer via C–C coupling reaction, Nature Chem. 9 (6) (2017) 563–570.
[10] K.-D. Zhang, J. Tian, D. Hanifi, Y. Zhang, A.C.-H. Sue, T.-Y. Zhou, L. Zhang, X. Zhao, Y. Liu, Z.-T. Li, Toward a single-layer two-dimensional honeycomb supramolecular organic framework in water, J. Am. Chem. Soc. 135 (47) (2013) 17913–17918.
[11] J. Xu, J. Mahmood, Y. Dou, S. Dou, F. Li, L. Dai, J.-B. Baek, 2D frameworks of C2N and C3N as new anode materials for lithium-ion batteries, Adv. Mater. 29 (2017) 1702007–1702015.
[12] Y. Suzuki, G. Cardone, D. Restrepo, P.D. Zavattieri, T.S. Baker, F.A. Tezcan, Self-assembly of coherently dynamic, auxetic, two-dimensional protein crystals, Nature 533 (7603) (2016) 369–373.
[13] T. Jiang, C. Xu, Y. Liu, Z. Liu, J.S. Wall, X. Zuo, T. Lian, K. Salaita, C. Ni, D. Pochan, V.P. Conticello, Structurally defined nanoscale sheets from self-assembly of collagen-mimetic peptides, J. Am. Chem. Soc. 136 (11) (2014) 4300–4308.
[14] J.D. Brodin, X.I. Ambroggio, C. Tang, K.N. Parent, T.S. Baker, F.A. Tezcan, Metal-directed, chemically tunable assembly of one-, two- and three-dimensional crystalline protein arrays, Nature Chem. 4 (5) (2012) 375–382.
[15] W. Liu, H. Zhong, R. Wang, N.C. Seeman, Crystalline two-dimensional DNA-origami arrays, Angew. Chem. Int. Ed. 50 (1) (2011) 264–267.
[16] H. Jin, F. Jiao, M.D. Daily, Y. Chen, F. Yan, Y.-H. Ding, X. Zhang, E.J. Robertson, M.D. Baer, C.-L. Chen, Highly stable and self-repairing membrane-mimetic 2D nanomaterials assembled from lipid-like peptoids, Nature Commun. (7) (2016) 12252.
[17] F. Jiao, Y. Chen, H. Jin, P. He, C.-L. Chen, J.J. De Yoreo, Self-repair and patterning of 2D membrane-like peptoid materials, Adv. Funct. Mater. (26) (2016) 8960–8967.
[18] P. Wang, S. Gaitanaros, S. Lee, M. Bathe, W.M. Shih, Y. Ke, Programming self-assembly of DNA origami honeycomb two-dimensional lattices and plasmonic metamaterials, J. Am. Chem. Soc. 138 (24) (2016) 7733–7740.
[19] Y. Suzuki, M. Endo, H. Sugiyama, Lipid-bilayer-assisted two-dimensional self-assembly of dna origami nanostructures, Nature Commun. 6 (2015).
[20] F. Hong, F. Zhang, Y. Liu, H. Yan, DNA Origami: Scaffolds for creating higher order structures, Chem. Rev. (2017).
[21] A.V. Pinheiro, D.R. Han, W.M. Shih, H. Yan, Challenges and opportunities for structural DNA nanotechnology, Nat. Nanotechnol. 6 (12) (2011) 763–772.
[22] T. Torring, N.V. Voigt, J. Nangreave, H. Yan, K.V. Gothelf, DNA origami: a quantum leap for self-assembly of complex structures, Chem. Soc. Rev. 40 (12) (2011) 5636–5646.
[23] U.B. Sleytr, T.J. Beveridge, Bacterial S-layers, Trends Microbiol. 7 (6) (1999) 253–260.
[24] S. Gonen, F. DiMaio, T. Gonen, D. Baker, Design of ordered two-dimensional arrays mediated by noncovalent protein-protein interfaces, Science 348 (6241) (2015) 1365–1368.
[25] A. Fegan, B. White, J.C.T. Carlson, C.R. Wagner, Chemically controlled protein assembly: Techniques and applications, Chem. Rev. 110 (6) (2010) 3315–3336.
[26] E.N. Salgado, R.J. Radford, F.A. Tezcan, Metal-directed protein self-assembly, Acc. Chem. Res. 43 (5) (2010) 661–672.
[27] I. Drobnak, A. Ljubetič, H. Gradišar, T. Pisanski, R. Jerala, Designed protein origami, in: A.L. Cortajarena, T.Z. Grove (Eds.), Protein-based Engineered Nanostructures, Springer International Publishing, Cham, 2016, pp. 7–27.
[28] Q. Luo, C. Hou, Y. Bai, R. Wang, J. Liu, Protein assembly: Versatile approaches to construct highly ordered nanostructures, Chem. Rev. 116 (22) (2016) 13571–13632.
[29] C.L. Chen, N.L. Rosi, Peptide-based methods for the preparation of nanostructured inorganic materials, Angew. Chem. Int. Ed. 49 (11) (2010) 1924–1942.
[30] H. Cui, M.J. Webber, S.I. Stupp, Self-assembly of peptide amphiphiles: from molecules to nanostructures to biomaterials, Biopolymers 94 (1) (2010) 1–18.
[31] R.V. Ulijn, A.M. Smith, Designing peptide based nanomaterials, Chem. Soc. Rev. 37 (4) (2008) 664–675.
[32] I.W. Hamley, A. Dehsorkhi, V. Castelletto, Self-assembled arginine-coated peptide nanosheets in water, Chem. Commun. 49 (18) (2013) 1850–1852.
[33] B. Dai, D. Li, W. Xi, F. Luo, X. Zhang, M. Zou, M. Cao, J. Hu, W. Wang, G. Wei, Y. Zhang, C. Liu, Tunable assembly of amyloid-forming peptides into nanosheets as a retrovirus carrier, Proc. Natl. Acad. Sci. USA 112 (10) (2015) 2996–3001.
[34] M. Hughes, H. Xu, P.W.J.M. Frederix, A.M. Smith, N.T. Hunt, T. Tuttle, I.A. Kinloch, R.V. Ulijn, Biocatalytic self-assembly of 2D peptide-based nanostructures, Soft Matter 7 (21) (2011) 10032–10038.
[35] M.J. Buehler, Y.C. Yung, Deformation and failure of protein materials in physiologically extreme conditions and disease, Nature Mater. 8 (3) (2009) 175–188.
[36] J. Sun, R.N. Zuckermann, Peptoid polymers: a highly designable bioinspired material, ACS Nano 7 (6) (2013) 4715–4732.
[37] C.L. Chen, R.N. Zuckermann, J.J. DeYoreo, Surface-directed assembly of sequence defined synthetic polymers into networks of hexagonally patterned nanoribbons with controlled functionalities, ACS Nano 10 (5) (2016) 5314–5320.
[38] X. Ma, S. Zhang, F. Jiao, C.J. Newcomb, Y. Zhang, A. Prakash, Z. Liao, M.D. Baer, C.J. Mundy, J. Pfaendtner, A. Noy, C.-L. Chen, J.J. De Yoreo, Tuning crystallization pathways through sequence engineering of biomimetic polymers, Nature Mater. 16 (2017) 767–775.
[39] K.T. Nam, S.A. Shelby, P.H. Choi, A.B. Marciel, R. Chen, L. Tan, T.K. Chu, R.A. Mesch, B.-C. Lee, M.D. Connolly, C. Kisielowski, R.N. Zuckermann, Free-floating ultrathin two-dimensional crystals from sequence-specific peptoid polymers, Nature Mater. 9 (5) (2010) 454–460.
[40] T.K. Haxton, R.V. Mannige, R.N. Zuckermann, S. Whitelam, Modeling sequence-specific polymers using anisotropic coarse-grained sites allows quantitative comparison with experiment, J. Chem. Theory Comput. 11 (1) (2015) 303–315.
[41] E.J. Robertson, G.K. Oliver, M. Qian, C. Proulx, R.N. Zuckermann, G.L. Richmond, Assembly and molecular order of two-dimensional peptoid nanosheets through the oil-water interface, Proc. Natl. Acad. Sci. USA 111 (37) (2014) 13284–13289.

[42] B. Sanii, R. Kudirka, A. Cho, N. Venkateswaran, G.K. Olivier, A.M. Olson, H. Tran, R.M. Harada, L. Tan, R.N. Zuckermann, Shaken, not stirred: collapsing a peptoid monolayer to produce free-floating, stable nanosheets, J. Am. Chem. Soc. 133 (51) (2011) 20808–20815.
[43] B. Sanii, T.K. Haxton, G.K. Olivier, A. Cho, B. Barton, C. Proulx, S. Whitelam, R.N. Zuckermann, Structure-determining step in the hierarchical assembly of peptoid nanosheets, ACS Nano 8 (11) (2014) 11674–11684.
[44] R. Kudirka, H. Tran, B. Sanii, N. Ki Tae, P.H. Choi, N. Venkateswaran, R. Chen, S. Whitelam, R.N. Zuckermann, Folding of a single-chain, information-rich polypeptoid sequence into a highly ordered nanosheet, Biopolymers 96 (5) (2011) 586–595.
[45] E.J. Robertson, C. Proulx, J.K. Su, R.L. Garcia, S. Yoo, E.M. Nehls, M.D. Connolly, L. Taravati, R.N. Zuckermann, Molecular engineering of the peptoid nanosheet hydrophobic core, Langmuir 32 (45) (2016) 11946–11957.
[46] M.D. Karkas, E.V. Johnston, O. Verho, B. Akermark, Artificial photosynthesis: photosynthesis: from nanosecond electron transfer to catalytic water oxidation, Acc. Chem. Res. 47 (1) (2014) 100–111.
[47] C. Shih, A.K. Museth, M. Abrahamsson, A.M. Blanco-Rodriguez, A.J. Di Bilio, J. Sudhamsu, B.R. Crane, K.L. Ronayne, M. Towrie, A. Vlcek Jr., J.H. Richards, J.R. Winkler, H.B. Gray, Tryptophan-accelerated electron flow through proteins, Science 320 (5884) (2008) 1760–1762.
[48] A. Natansohn, P. Rochon, Photoinduced motions in azo-containing polymers, Chem. Rev. 102 (11) (2002) 4139–4175.
[49] M.-C. Kim, S.-Y. Lee, Carbonic anhydrase-mimetic bolaamphiphile self-assembly for CO2 hydration and sequestration, Chem. Eur. J. 20 (51) (2014) 17019–17024.
[50] J.D. Brodin, J.R. Carr, P.A. Sontz, F.A. Tezcan, Exceptionally stable, redox-active supramolecular protein assemblies with emergent properties, Proc. Natl. Acad. Sci. USA 111 (8) (2014) 2897–2902.
[51] J.M.V. Jun, M.V.P. Altoe, S. Aloni, R.N. Zuckermann, Peptoid nanosheets as soluble, two-dimensional templates for calcium carbonate mineralization, Chem. Commun. 51 (50) (2015) 10218–10221.
[52] H.S. Jang, J.H. Lee, Y.S. Park, Y.O. Kim, J. Park, T.Y. Yang, K. Jin, J. Lee, S. Park, J.M. You, K.W. Jeong, A. Shin, I.S. Oh, M.K. Kwon, Y.I. Kim, H.H. Cho, H.N. Han, Y. Kim, Y.H. Chang, S.R. Paik, K.T. Nam, Y.S. Lee, Tyrosine-mediated two-dimensional peptide assembly and its role as a bio-inspired catalytic scaffold, Nature Commun. 5 (2014).
[53] M. Yolamanova, C. Meier, A.K. Shaytan, V. Vas, C.W. Bertoncini, F. Arnold, O. Zirafi, S.M. Usmani, J.A. Muller, D. Sauter, C. Goffinet, D. Palesch, P. Walther, N.R. Roan, H. Geiger, O. Lunov, T. Simmet, J. Bohne, H. Schrezenmeier, K. Schwarz, L. Standker, W.-G. Forssmann, X. Salvatella, P.G. Khalatur, A.R. Khokhlov, T.P.J. Knowles, T. Weil, F. Kirchhoff, J. Munch, Peptide nanofibrils boost retroviral gene transfer and provide a rapid means for concentrating viruses, Nat. Nano 8 (2) (2013) 130–136.
[54] G.K. Olivier, A. Cho, B. Sanii, M.D. Connolly, H. Tran, R.N. Zuckermann, Antibody-mimetic peptoid nanosheets for molecular recognition, ACS Nano 7 (10) (2013) 9276–9286.
[55] M.M. Reddy, R. Wilson, J. Wilson, S. Connell, A. Gocke, L. Hynan, D. German, T. Kodadek, Identification of candidate IgG biomarkers for alzheimer's disease via combinatorial library screening, Cell 144 (1) (2011) 132–142.
[56] L. Zhu, Z. Zhao, P. Cheng, Z. He, Z. Cheng, J. Peng, H. Wang, C. Wang, Y. Yang, Z. Hu, Antibody-mimetic peptoid nanosheet for label-free serum-based diagnosis of alzheimer's disease, Adv. Mater. 29 (30) (2017). http://dx.doi.org/10.1002/adma.201700057.
[57] J.J. De Yoreo, N. Sommerdijk, Investigating materials formation with liquid-phase and cryogenic TEM, Nat. Rev. Mater. 1 (8) (2016).
[58] R.V. Mannige, T.K. Haxton, C. Proulx, E.J. Robertson, A. Battigelli, G.L. Butterfoss, R.N. Zuckermann, S. Whitelam, Peptoid nanosheets exhibit a new secondary-structure motif, Nature 526 (7573) (2015) 415–420.
[59] P.-S. Huang, S.E. Boyken, D. Baker, The coming of age of de novo protein design, Nature 537 (7620) (2016) 320–327.